

## The sputtering of radioactive recoil nuclides induced by fast neutron

Bangjiao Ye, Yoshimi Kasugai, Yujiro Ikeda, Yangmei Fan, Xianyi Zhou, Jiangfeng Du, and Rongdian Han

Citation: *Journal of Applied Physics* **87**, 2581 (2000); doi: 10.1063/1.372222

View online: <http://dx.doi.org/10.1063/1.372222>

View Table of Contents: <http://scitation.aip.org/content/aip/journal/jap/87/5?ver=pdfcov>

Published by the [AIP Publishing](#)

---

### Articles you may be interested in

[Simultaneous impact of neutron irradiation and sputtering on the surface structure of self-damaged ITER-grade tungsten](#)

*AIP Advances* **4**, 077121 (2014); 10.1063/1.4890594

[Effect of fast neutron irradiation induced defects on the metamagnetic transition in Ce\(Fe<sub>0.96</sub>Ru<sub>0.04</sub>\)<sub>2</sub>](#)

*J. Appl. Phys.* **112**, 063922 (2012); 10.1063/1.4754577

[Facility for fast neutron irradiation tests of electronics at the ISIS spallation neutron source](#)

*Appl. Phys. Lett.* **92**, 114101 (2008); 10.1063/1.2897309

[Neutron production by fast protons from ultraintense laser-plasma interactions](#)

*J. Appl. Phys.* **96**, 6912 (2004); 10.1063/1.1814421

[Neutron capture therapy \(NCT\) enhancement of fast neutron radiotherapy: Application to non-small cell lung cancer](#)

*AIP Conf. Proc.* **576**, 881 (2001); 10.1063/1.1395444

---



# The sputtering of radioactive recoil nuclides induced by fast neutron

Bangjiao Ye<sup>a)</sup>

University of Science and Technology of China, Hefei, Anhui 230027, People's Republic of China

Yoshimi Kasugai<sup>b)</sup> and Yujiro Ikeda

Japan Atomic Energy Research Institute, Tokai-mura, Ibaraki-gun, Japan

Yangmei Fan, Xianyi Zhou, Jiangfeng Du, and Rongdian Han

University of Science and Technology of China, Hefei, Anhui 230027, People's Republic of China

(Received 10 November 1998; accepted for publication 8 November 1999)

The sputtering of radioactive recoil nuclides in nonelastic reactions induced by 14.9 MeV neutrons has been studied by both the theoretical calculation and the experimental measurement. The sputtering yields of recoil nuclides have been calculated for nonelastic neutron reaction based on the nuclear reaction dynamic and sputtering theory. Systematics of reduced sputtering yields depending on the mass number of recoil nuclides have been found for  $(n,2n)$ ,  $(n,p)$ ,  $(n,\alpha)$  and  $(n,np)$  reactions. These systematics have also been demonstrated in the experimental measurement. Based on the differences of the calculating results and experimental ones, a universal revised calculating formula is presented for predicting the reduced sputtering yields induced by fast neutrons. © 2000 American Institute of Physics. [S0021-8979(00)04704-6]

## I. INTRODUCTION

When energetic particles bombard a solid and the energy is transferred to a surface or a near surface atom, sputtering can occur. Neutron sputtering, i.e., the removal of atoms (or clusters and microsize particles) from the surfaces during neutron bombardment, is an important process in connection with radiation damage mechanism and ranges of energetic ions in a solid. In a fusion power reactor, the walls of the vacuum vessel containing the plasma will be bombarded by very high power levels of 14 MeV neutrons. For example, according to the design report of the International Thermonuclear Experimental Reactor (ITER), the average neutron load is about 1–2 MW/m<sup>2</sup>. The actual neutron flux may be much higher than the 14 MeV source flux due to scattering and nuclear reactions in the blanket. Neutron sputtering will introduce atoms from the solid wall of the plasma chamber into the hot deuterium–tritium plasma<sup>1</sup> and lead to emit radioactive wall atoms into the coolants of the cooling system.<sup>2</sup> Neutron sputtering will also contribute to erosion of the vessel walls.<sup>3</sup>

Most of the experimental measurements and theoretical treatments for neutron sputtering yields were carried out during the 1970s. After that time, there were almost no data in the literature on the fast neutron induced recoil sputtering yields. Unfortunately, the neutron sputtering yields are still poorly investigated. The experimental data on the neutron sputtering yield is very scarce and contradictory. Different measurements on Nb, for example, had different results in wide scattering in the sputtering yields<sup>4,5</sup> and had large differences with the results predicted by theory.<sup>6,7</sup> Usually, the

experimental data were much higher than the theoretical predictions.<sup>8,9</sup> The highest reported sputtering yields have been associated with the observation of micron sized “chunks” of target material.<sup>10–12</sup> If the higher sputtering ratios were correct, neutron sputtering would be a critical issue for the fusion reactors.

Neutron sputtering of near surface target will be dominated by elastic neutron scattering mainly through the production of recoil cascades of target atoms produced by high energy primary recoils from fast neutron scattering. This process was described well in sputtering theory by Sigmund.<sup>13</sup> But in the experiment to measure sputtering yields induced by elastic neutron scattering is very difficult. In this article, the authors first make a calculation on sputtering yields ( $S_n$ ) of radioactive recoil nuclides by nonelastic neutron reactions based on neutron sputtering theory<sup>12</sup> and nuclear reaction dynamics. In order to analyze a probable systematics, a reduced sputtering yield ( $RS_n$ ) is introduced. Based on a large number calculating results, the systematics of  $RS_n$  have been

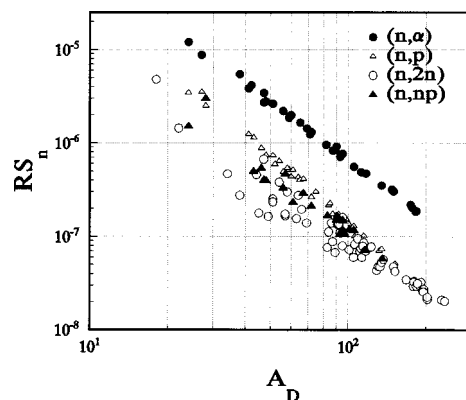


FIG. 1. Systematics of calculating  $RS_n$  for  $(n,2n)$ ,  $(n,p)$ ,  $(n,\alpha)$  and  $(n,np)$  reactions.

<sup>a)</sup>Author to whom correspondence should be addressed; electronic mail: bjye@ustc.edu.cn

<sup>b)</sup>Present address: Neutron Science Center, Japan Atomic Energy Research Institute, Tokai-mura, Ibaraki-gun, Japan.

TABLE I. The  $RS_n$  values of various reactions for different target materials.

Material	Z	$RS_n(1/\text{barn})$							$\sigma(b)$	
		(n,2n)	(n,p)	(n, $\alpha$ )	(n,np)	(n,non.)	(n,n)	(n,total)	(n,tot)	(n,n)
<sup>19</sup> F	9	$1.20 \times 10^{-5}$	$1.56 \times 10^{-5}$	$1.98 \times 10^{-5}$	$2.98 \times 10^{-5}$	$2.16 \times 10^{-5}$	$4.48 \times 10^{-5}$	$3.55 \times 10^{-5}$	1.741	1.046
<sup>24</sup> Mg	12	$4.31 \times 10^{-6}$	$5.87 \times 10^{-6}$	$8.56 \times 10^{-6}$	$9.58 \times 10^{-6}$	$7.09 \times 10^{-6}$	$1.59 \times 10^{-6}$	$9.91 \times 10^{-6}$	1.798	0.575
<sup>27</sup> Al	13	$3.24 \times 10^{-6}$	$4.48 \times 10^{-6}$	$6.78 \times 10^{-6}$	$6.99 \times 10^{-6}$	$5.20 \times 10^{-6}$	$1.19 \times 10^{-5}$	$8.31 \times 10^{-6}$	1.72	0.798
<sup>28</sup> Si	14	$2.49 \times 10^{-6}$	$3.48 \times 10^{-6}$	$5.46 \times 10^{-6}$	$5.21 \times 10^{-6}$	$3.90 \times 10^{-6}$	$9.12 \times 10^{-6}$	$6.16 \times 10^{-6}$	1.761	0.758
<sup>41</sup> K	19	$8.42 \times 10^{-7}$	$1.24 \times 10^{-6}$	$2.24 \times 10^{-6}$	$1.56 \times 10^{-6}$	$1.19 \times 10^{-6}$	$3.04 \times 10^{-6}$	$2.08 \times 10^{-6}$	2.084	1.001
<sup>43</sup> Ca	20	$7.02 \times 10^{-7}$	$1.04 \times 10^{-6}$	$1.93 \times 10^{-6}$	$1.28 \times 10^{-6}$	$9.79 \times 10^{-7}$	$2.53 \times 10^{-6}$	$1.74 \times 10^{-6}$	2.396	1.175
<sup>45</sup> Sc	21	$5.90 \times 10^{-7}$	$8.81 \times 10^{-7}$	$1.68 \times 10^{-6}$	$1.05 \times 10^{-6}$	$8.11 \times 10^{-7}$	$2.12 \times 10^{-6}$	$1.51 \times 10^{-6}$	2.175	1.159
<sup>48</sup> Ti	22	$5.00 \times 10^{-7}$	$7.53 \times 10^{-7}$	$1.46 \times 10^{-6}$	$8.75 \times 10^{-7}$	$6.77 \times 10^{-7}$	$1.79 \times 10^{-6}$	$1.16 \times 10^{-6}$	2.372	1.036
<sup>51</sup> V	23	$4.27 \times 10^{-7}$	$6.48 \times 10^{-7}$	$1.29 \times 10^{-6}$	$7.34 \times 10^{-7}$	$5.70 \times 10^{-7}$	$1.53 \times 10^{-6}$	$9.85 \times 10^{-7}$	2.35	1.018
<sup>52</sup> Cr	24	$3.67 \times 10^{-7}$	$5.61 \times 10^{-7}$	$1.14 \times 10^{-6}$	$6.21 \times 10^{-7}$	$4.83 \times 10^{-7}$	$1.31 \times 10^{-6}$	$8.35 \times 10^{-7}$	2.419	1.029
<sup>55</sup> Mn	25	$3.18 \times 10^{-7}$	$4.88 \times 10^{-7}$	$1.01 \times 10^{-6}$	$5.28 \times 10^{-7}$	$4.13 \times 10^{-7}$	$1.13 \times 10^{-6}$	$7.52 \times 10^{-7}$	2.568	1.214
<sup>56</sup> Fe	26	$2.76 \times 10^{-7}$	$4.27 \times 10^{-7}$	$8.99 \times 10^{-7}$	$4.52 \times 10^{-7}$	$3.54 \times 10^{-7}$	$9.82 \times 10^{-7}$	$6.32 \times 10^{-7}$	2.574	1.137
<sup>59</sup> Co	27	$2.42 \times 10^{-7}$	$3.76 \times 10^{-7}$	$8.05 \times 10^{-7}$	$3.90 \times 10^{-7}$	$3.06 \times 10^{-7}$	$8.58 \times 10^{-7}$	$5.69 \times 10^{-7}$	2.653	1.265
<sup>58</sup> Ni	28	$2.12 \times 10^{-7}$	$3.32 \times 10^{-7}$	$7.24 \times 10^{-7}$	$3.38 \times 10^{-7}$	$2.66 \times 10^{-7}$	$7.52 \times 10^{-7}$	$5.03 \times 10^{-7}$	2.664	1.297
<sup>64</sup> Zn <sup>a</sup>	30	$1.66 \times 10^{-7}$	$2.63 \times 10^{-7}$	$5.92 \times 10^{-7}$	$2.57 \times 10^{-7}$	$2.04 \times 10^{-7}$	$5.87 \times 10^{-7}$	$3.94 \times 10^{-7}$	3.057	1.52
<sup>65</sup> Cu	29	$1.87 \times 10^{-7}$	$2.95 \times 10^{-7}$	$6.54 \times 10^{-7}$	$2.94 \times 10^{-7}$	$2.32 \times 10^{-7}$	$6.63 \times 10^{-7}$	$4.42 \times 10^{-7}$	2.914	1.418
<sup>74</sup> Ge	32	$1.32 \times 10^{-7}$	$2.11 \times 10^{-7}$	$4.91 \times 10^{-7}$	$1.99 \times 10^{-7}$	$1.59 \times 10^{-7}$	$4.65 \times 10^{-7}$	$3.17 \times 10^{-7}$	3.274	1.694
<sup>75</sup> As	33	$1.18 \times 10^{-7}$	$1.91 \times 10^{-7}$	$4.49 \times 10^{-7}$	$1.77 \times 10^{-7}$	$1.41 \times 10^{-7}$	$4.16 \times 10^{-7}$	$2.83 \times 10^{-7}$	3.457	1.778
<sup>88</sup> Sr	38	$7.17 \times 10^{-8}$	$1.18 \times 10^{-7}$	$2.97 \times 10^{-7}$	$1.01 \times 10^{-7}$	$8.14 \times 10^{-8}$	$2.51 \times 10^{-7}$	$1.92 \times 10^{-7}$	4.335	2.827
<sup>90</sup> Zr	40	$5.98 \times 10^{-8}$	$9.93 \times 10^{-8}$	$2.56 \times 10^{-7}$	$8.26 \times 10^{-8}$	$6.68 \times 10^{-8}$	$2.08 \times 10^{-7}$	$1.54 \times 10^{-7}$	4.336	2.673
<sup>93</sup> Nb	41	$5.48 \times 10^{-8}$	$9.13 \times 10^{-8}$	$2.38 \times 10^{-7}$	$7.49 \times 10^{-8}$	$6.07 \times 10^{-8}$	$1.91 \times 10^{-7}$	$1.33 \times 10^{-7}$	3.973	2.223
<sup>96</sup> Mo	42	$5.03 \times 10^{-8}$	$8.41 \times 10^{-8}$	$2.22 \times 10^{-7}$	$6.81 \times 10^{-8}$	$5.53 \times 10^{-8}$	$1.75 \times 10^{-7}$	$1.26 \times 10^{-7}$	4.339	2.559
<sup>102</sup> Ru	44	$4.26 \times 10^{-8}$	$7.19 \times 10^{-8}$	$1.94 \times 10^{-7}$	$5.67 \times 10^{-8}$	$4.61 \times 10^{-8}$	$1.48 \times 10^{-7}$	$1.02 \times 10^{-7}$	4.536	2.485
<sup>110</sup> Pd	46	$3.64 \times 10^{-8}$	$6.18 \times 10^{-8}$	$1.70 \times 10^{-7}$	$4.76 \times 10^{-8}$	$3.88 \times 10^{-8}$	$1.26 \times 10^{-7}$	$8.53 \times 10^{-8}$	4.477	2.387
<sup>107</sup> Ag	47	$3.37 \times 10^{-8}$	$5.75 \times 10^{-8}$	$1.60 \times 10^{-7}$	$4.37 \times 10^{-8}$	$3.57 \times 10^{-8}$	$1.17 \times 10^{-7}$	$8.35 \times 10^{-8}$	4.26	2.514
<sup>116</sup> Cd	48	$3.13 \times 10^{-8}$	$5.35 \times 10^{-8}$	$1.51 \times 10^{-7}$	$4.02 \times 10^{-8}$	$3.29 \times 10^{-8}$	$1.08 \times 10^{-7}$	$7.51 \times 10^{-8}$	4.475	2.512
<sup>115</sup> In	49	$2.91 \times 10^{-8}$	$4.99 \times 10^{-8}$	$1.42 \times 10^{-7}$	$3.71 \times 10^{-8}$	$3.04 \times 10^{-8}$	$1.00 \times 10^{-7}$	$7.48 \times 10^{-8}$	4.635	2.944
<sup>120</sup> Sn	50	$2.71 \times 10^{-8}$	$4.66 \times 10^{-8}$	$1.34 \times 10^{-7}$	$3.42 \times 10^{-8}$	$2.81 \times 10^{-8}$	$9.33 \times 10^{-8}$	$6.93 \times 10^{-8}$	4.636	2.928
<sup>138</sup> Ba	56	$1.81 \times 10^{-8}$	$3.17 \times 10^{-8}$	$9.61 \times 10^{-8}$	$2.19 \times 10^{-8}$	$1.81 \times 10^{-8}$	$6.21 \times 10^{-8}$	$4.31 \times 10^{-8}$	5.078	2.889
<sup>142</sup> Nd	60	$1.42 \times 10^{-8}$	$2.51 \times 10^{-8}$	$7.86 \times 10^{-8}$	$1.67 \times 10^{-8}$	$1.39 \times 10^{-8}$	$4.84 \times 10^{-8}$	$3.44 \times 10^{-8}$	4.781	2.842
<sup>153</sup> Eu	63	$1.19 \times 10^{-8}$	$2.13 \times 10^{-8}$	$6.81 \times 10^{-8}$	$1.37 \times 10^{-8}$	$1.15 \times 10^{-8}$	$4.06 \times 10^{-8}$	$2.75 \times 10^{-8}$	5.20	2.865
<sup>158</sup> Gd	64	$1.13 \times 10^{-8}$	$2.02 \times 10^{-8}$	$6.51 \times 10^{-8}$	$1.29 \times 10^{-8}$	$1.08 \times 10^{-8}$	$3.84 \times 10^{-8}$	$2.74 \times 10^{-8}$	5.694	3.423
<sup>159</sup> Tb	65	$1.07 \times 10^{-8}$	$1.92 \times 10^{-8}$	$6.22 \times 10^{-8}$	$1.21 \times 10^{-8}$	$1.02 \times 10^{-8}$	$3.63 \times 10^{-8}$	$2.57 \times 10^{-8}$	5.258	3.116
<sup>165</sup> Ho <sup>b</sup>	67	$9.57 \times 10^{-9}$	$1.73 \times 10^{-8}$	$5.69 \times 10^{-8}$	$1.08 \times 10^{-8}$	$9.05 \times 10^{-9}$	$3.25 \times 10^{-8}$	$2.17 \times 10^{-8}$	5.322	2.875
<sup>175</sup> Lu <sup>b</sup>	71	$7.79 \times 10^{-9}$	$1.42 \times 10^{-8}$	$4.81 \times 10^{-8}$	$8.57 \times 10^{-9}$	$7.23 \times 10^{-9}$	$2.64 \times 10^{-8}$	$1.83 \times 10^{-8}$	5.257	3.021
<sup>180</sup> Hf	72	$7.41 \times 10^{-9}$	$1.35 \times 10^{-8}$	$4.62 \times 10^{-8}$	$8.11 \times 10^{-9}$	$6.84 \times 10^{-9}$	$2.51 \times 10^{-8}$	$1.62 \times 10^{-8}$	5.485	2.804
<sup>181</sup> Ta	73	$7.05 \times 10^{-9}$	$1.29 \times 10^{-8}$	$4.44 \times 10^{-8}$	$7.68 \times 10^{-9}$	$6.49 \times 10^{-9}$	$2.39 \times 10^{-8}$	$1.62 \times 10^{-8}$	5.37	2.991
<sup>184</sup> W	74	$6.72 \times 10^{-9}$	$1.23 \times 10^{-8}$	$4.26 \times 10^{-8}$	$7.28 \times 10^{-9}$	$6.16 \times 10^{-9}$	$2.28 \times 10^{-8}$	$1.42 \times 10^{-8}$	5.215	2.538
<sup>187</sup> Re	75	$6.41 \times 10^{-9}$	$1.18 \times 10^{-8}$	$4.10 \times 10^{-8}$	$6.90 \times 10^{-9}$	$5.84 \times 10^{-9}$	$2.17 \times 10^{-8}$	$1.39 \times 10^{-8}$	5.312	2.699
<sup>197</sup> Au <sup>b</sup>	79	$5.33 \times 10^{-9}$	$9.89 \times 10^{-9}$	$3.52 \times 10^{-8}$	$5.62 \times 10^{-9}$	$4.78 \times 10^{-9}$	$1.80 \times 10^{-8}$	$1.14 \times 10^{-8}$	5.305	2.64
<sup>208</sup> Pb	82	$4.67 \times 10^{-9}$	$8.72 \times 10^{-9}$	$3.16 \times 10^{-8}$	$4.85 \times 10^{-9}$	$4.14 \times 10^{-9}$	$1.57 \times 10^{-8}$	$9.34 \times 10^{-9}$	5.364	2.41
<sup>209</sup> Bi	83	$4.47 \times 10^{-9}$	$8.36 \times 10^{-9}$	$3.05 \times 10^{-8}$	$4.62 \times 10^{-9}$	$3.95 \times 10^{-9}$	$1.51 \times 10^{-8}$	$9.75 \times 10^{-9}$	5.37	2.804

<sup>a</sup>Data of cross section of JEF 2.2 was used.<sup>b</sup>Data of cross section of ENDF/B-VI was used.

TABLE II. The fitting parameters  $a$  and  $b$  for calculating  $RS_n$ .

Reactions	$a$	$b$
$(n,2n)$	0.000 314	-1.7774
$(n,p)$	0.009 090	-2.4148
$(n,\alpha)$	0.007 960	-2.0414
$(n,np)$	0.001 318	-2.0383

found for  $(n,2n)$ ,  $(n,p)$ ,  $(n,\alpha)$  and  $(n,np)$  reactions. These systematics have also been demonstrated in the experimental measurement, which was finished at the Fusion Neutronics Source (FNS) laboratory, Japan Atomic Energy Research Institute (JAERI). Moreover, based the experimental results, a revised calculating formula is deduced to predict  $RS_n$  of various reactions.

**II. SYSTEMATICS OF REDUCED SPUTTERING YIELDS I, THEORETICAL CALCULATION**

In the sputtering process induced by fast neutrons, the primary knock on atoms can be produced in a nuclear non-elastic reaction such as  $(n,2n)$ ,  $(n,p)$ ,  $(n,\alpha)$ ,  $(n,np)$ , etc. For a reaction  $C(n,b)D$ , where  $C$ ,  $D$ ,  $n$  and  $b$  are target nuclide, recoil nuclide, incident neutron and light particles, respectively, according to the mechanics of nuclear reaction, the kinetic energy of the recoil nuclide,  $T$ , in the laboratory coordinate system, is

$$T = \left\{ \frac{(A_D E_n)^{1/2}}{(A_D + A_b)} \cos \theta \pm \left( \frac{A_D E_n}{(A_D + A_b)^2} \cos^2 \theta + \frac{A_b Q + (A_b - 1) E_n}{(A_D + A_b)} \right)^{1/2} \right\}^2, \tag{1}$$

where  $A_D$  and  $A_b$  are the mass numbers of the recoil nuclides and the light ejected particles.  $E_n$  is the energy of incident neutron,  $Q$  is the reaction  $Q$  value, and  $\theta$  is the recoil nuclide

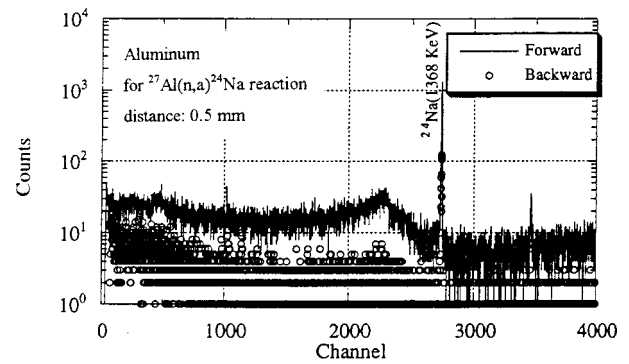


FIG. 3. Gamma-ray spectra from the collector for  $^{27}\text{Al}(n,\alpha)^{24}\text{Na}$  reaction.

scattering angle in the laboratory frame of reference. When  $\theta=0$ , the  $T$  is maximum recoil kinetic energy.

The average kinetic energy of the recoil nuclide is roughly estimated by average scattering angle  $\theta$

$$\bar{T} = \frac{A_D E_n}{(A_D + A_b)^2} + \frac{A_b Q + (A_b - 1) E_n}{A_D + A_b}. \tag{2}$$

The recoil nuclide starting with a kinetic energy  $T$  in the direction  $\theta$  of the neutron may have a range distribution  $F_R(T, \theta, x) dx$  in the direction  $x$  normal to the surface. If they start, which are uniformly distributed, in the solid, if the thickness  $c$  is much larger than the mean range, the sputtering yields in the forward directions are given<sup>12</sup>

$$S_n(E_n, \theta) = \frac{N}{\cos \theta} \sigma(E_n) \int_0^\infty x F_R(T, \theta, x) dx, \tag{3}$$

where  $\sigma(E_n)$  is the cross section of reaction between the incoming neutron and the target nuclide,  $N$  is the number density of atoms in the solid. Moreover, the surface potential is neglected, because we assume that the majority of the atoms arrive at the surface with much higher energies. The

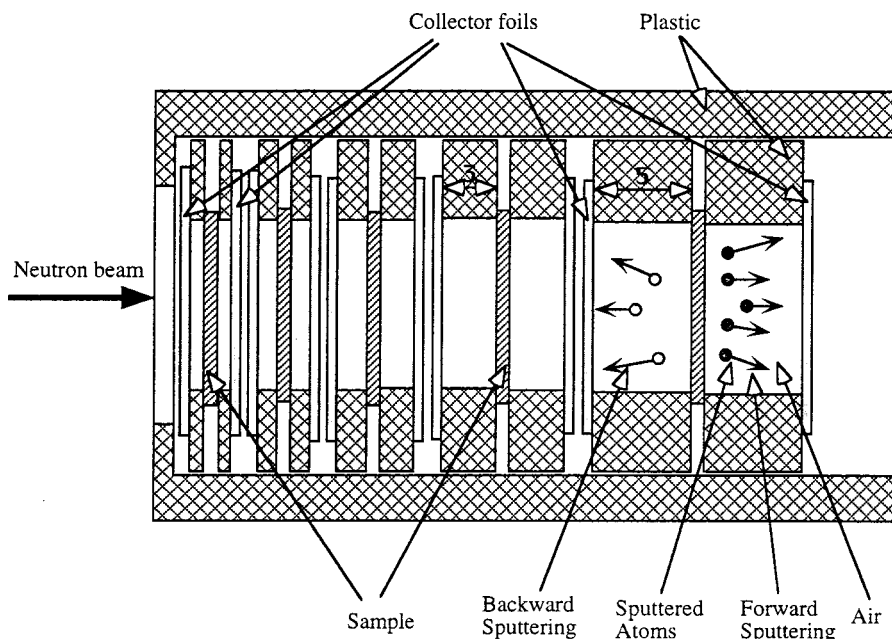


FIG. 2. Sample-collector assembly in measurement of neutron sputtering yields.

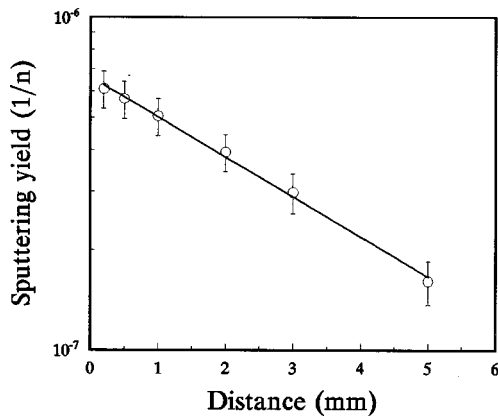


FIG. 4. Forward sputtering yields of different distances for  $^{27}\text{Al}(n,\alpha)^{24}\text{Na}$  reaction.

mean projected range of a recoil nuclide starting with  $T$  in a solid in the direction  $\theta$  relative to the surface normal is given by

$$\langle R(T, \theta) \rangle = \frac{\int_0^\infty x F_R(T, \theta, x) dx}{\int_0^\infty F_R(T, \theta, x) dx} \quad (4)$$

For nearly perpendicular neutron incidence, the denominator is close to one. For single-energy neutrons we get for the forward emission yield of recoil nuclide

$$S_n = \sigma(E_n) N \langle R(T) \rangle. \quad (5)$$

In order to examine a probable systematics for the sputtering yields, all  $S_n$  is divided by corresponding cross section values, which is defined as a reduced sputtering yields ( $RS_n$ ),

$$RS_n = \frac{S_n}{\sigma(\text{barn})}. \quad (6)$$

The reduced sputtering yields is obtained as follows according to Eqs. (5) and (6):

$$RS_n = N \langle R(T) \rangle. \quad (7)$$

In a practical calculation, usually, the kinetic energy  $T$  is replaced with the average kinetic energy  $\bar{T}$ . The theoretical

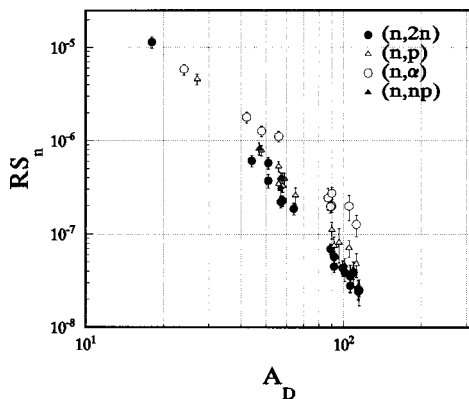


FIG. 5. Systematics of measuring  $RS_n$  for  $(n,2n)$ ,  $(n,p)$ ,  $(n,\alpha)$  and  $(n,np)$  reactions.

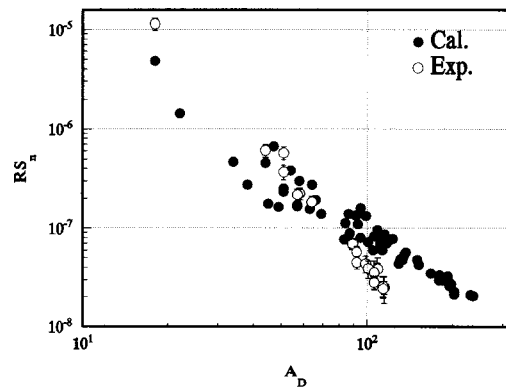


FIG. 6. Comparison of calculating and measuring  $RS_n$  for  $(n,2n)$  reaction.

mean ranges have been calculated using the results of Schott<sup>14</sup> for the low and intermediate energy ranges

$$\langle R(T) \rangle \left( \frac{\mu g}{\text{cm}^2} \right) = \begin{cases} C_i A_D \left( \frac{Z_C^{2/3} + Z_D^{2/3}}{Z_C Z_D} \bar{T}(\text{keV}) \right)^{2/3}, & \epsilon < 0.1, \\ C_i A_D \frac{(Z_C^{2/3} + Z_D^{2/3})^{1/2}}{Z_C Z_D} \bar{T}(\text{keV}), & 0.5 < \epsilon < 10 \end{cases} \quad (8)$$

where  $\epsilon$  is defined as a reduced energy

$$\epsilon = \frac{32.5 A_D}{(A_C + A_D) Z_C Z_D (Z_C^{2/3} + Z_D^{2/3})^{1/2}} T(\text{keV}), \quad (9)$$

where  $Z_C$  and  $Z_D$  are the atomic numbers of the target and the recoil nuclide, respectively,  $C_l$  and  $C_i$  are obtained from Figs. 4 and 7 of Schott.<sup>14</sup>

The  $RS_n$  of four kinds of nuclear reactions,  $(n,2n)$ ,  $(n,p)$ ,  $(n,\alpha)$  and  $(n,np)$ , are calculated. The results for 63 reactions of  $(n,2n)$  with  $Z$  from 9 to 92, 44 reactions of  $(n,p)$  with  $Z$  from 12 to 76, 32 reactions of  $(n,\alpha)$  with  $Z$  from 13 to 75 and 23 reactions of  $(n,np)$  with  $Z$  from 12 to 56 are obtained. The calculating results for some typical reactions are listed in Table I. According to calculating results, for the same target the  $RS_n$  of the  $(n,\alpha)$  reaction is the maximum and that of the  $(n,2n)$  reaction is minimum. The  $RS_n$  of four kinds of reactions are decreased with the in-

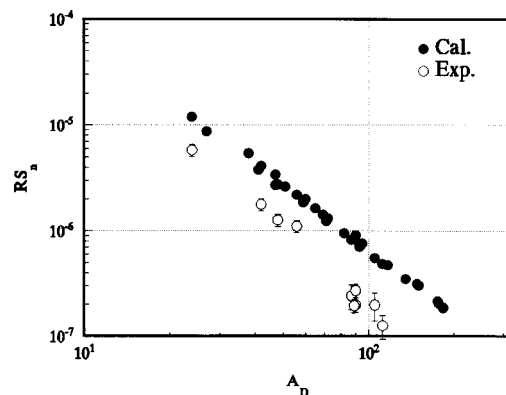


FIG. 7. Comparison of calculating and measuring  $RS_n$  for  $(n,\alpha)$  reaction.

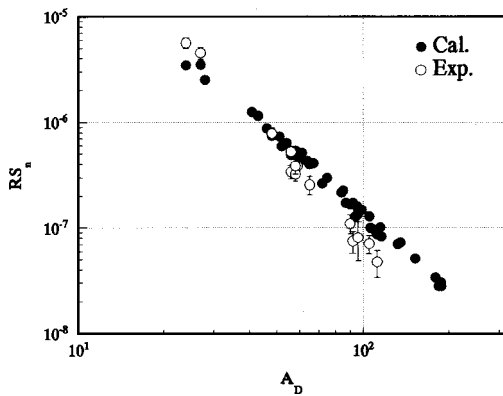


FIG. 8. Comparison of calculating and measuring  $RS_n$  for  $(n,p)$  reaction.

creasing of the mass number of recoil nuclide in an exponential form. A good systematics of  $RS_n$  depending on  $A_D$  is found for  $(n,p)$ ,  $(n,\alpha)$  and  $(n,np)$  reactions as shown in Fig. 1. For the  $(n,2n)$  reaction, there are some undulations for  $RS_n$  values at the range of  $A_D$  from 40 to 60 and the systematics is not as good as the other three kinds of reactions. The systematics of  $RS_n$  for four kinds of reactions can be given by

$$RS_n = aA_D^b, \tag{10}$$

where  $a$  and  $b$ , whose are given in the Table II are the fitting parameters.

### III. SYSTEMATICS OF REDUCED SPUTTERING YIELDS II, EXPERIMENTAL MEASUREMENT

Our experimental procedures<sup>15</sup> for measurement of neutron sputtering yield of emission of radioactive recoil nuclides are outlined in Fig. 2. The present measurement is performed in air. For this method, it needs to measure the change of the activity at the collector with the distance between the target and the collector. The collectors with 0.013 mm thickness are made from the plastic film. Most of the collectors are first cut into a  $2.5 \times 2.5 \text{ cm}^2$ . The surface of each collector is cleaned carefully. The range of the sputtering atoms is very short because of attenuation in the air. In the present measurement, several different distances between the target and the collector are used to deduce the function of

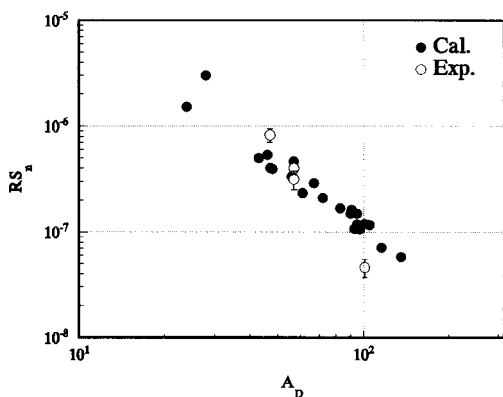


FIG. 9. Comparison of calculating and measuring  $RS_n$  for  $(n,np)$  reaction.

TABLE III. The fitting parameters  $a$  and  $b$  for experimental  $RS_n$ .

Reactions	$a$	$b$
$(n,2n)$	0.086 37	-3.1475
$(n,p)$	0.118 54	-3.1122
$(n,\alpha)$	0.022 53	-2.5445
$(n,np)$	1.159 98	-3.6980

sputtering yield varied with distances. For each sample five or six target-collector assemblies are prepared and mounted in a cylinder plastic tube. Each target-collector assembly consists of one target, two collectors and two plastic holders. The thicknesses of the holder are 0.2, 0.5, 1.0, 2.0, 3.0 and 5.0 mm, which separate the target from the collectors.

In the present experiment 24 materials of F, Mg, Al, Sc, Ti, V, Cr, Fe, Co, Ni, Cu, Zr, Nb, Mo, Pd, Ag, Cd, In, Ta, Rb, Pt, Au, Pb and SS316 are chosen to study the sputtering yields. The 14.9 MeV neutron is produced by a deuterium-tritium (DT) neutron generator at the FNS. The samples are irradiated in a rotational target room at an average neutron flux  $2.2 \times 10^{12} \text{ n/s}$  or in a fixed target room at the average neutron flux  $1.5 \times 10^{11} \text{ n/s}$ . The sample stack is placed at a distance of 10–50 mm from the neutron source in the direction of  $0^\circ$  to  $d^+$  beam. The irradiation time is changed according to the half lives of the recoil nuclide from 7 to 30 h, except for  $^{27}\text{Al}(n,p)^{27}\text{Mg}$  reaction for which only 10 min is used.

The sputtered radioactive materials deposited on the collectors are investigated by the neutron activation analysis. Four germanium detectors are used for gamma-ray measurement. The typical gamma-ray spectra from the collector for  $^{27}\text{Al}(n,\alpha)^{24}\text{Na}$  reaction is shown in Fig. 3. The neutron sputtering yields are obtained from the value of different positions for each sample for both forward and backward directions. The sputtering yield in the surface of the target investigated (0 mm) is deduced from extrapolation of the sputtering yields at the different distances. Figure 4 is an example for obtaining the forward sputtering yield of the  $^{27}\text{Al}(n,\alpha)^{24}\text{Na}$  reaction from those of different distances.

The reduced sputtering yields for 57 reactions, that is, 29, 10, 14 and 4 for  $(n,2n)$ ,  $(n,\alpha)$ ,  $(n,p)$  and  $(n,np)$ , respectively, are shown in Fig. 5. A systematics of  $RS_n$  de-

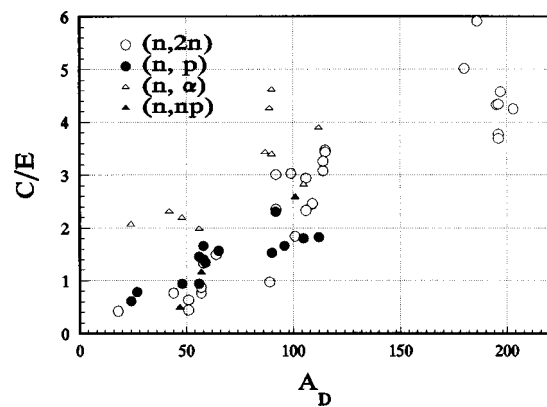


FIG. 10. Ratios between calculating and measuring  $RS_n$ .

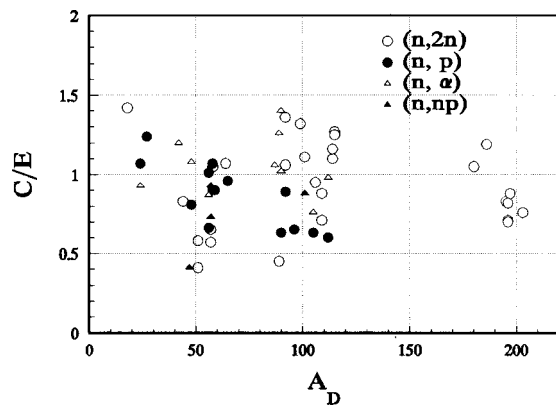


FIG. 11. New  $C/E$  values obtained by using revised calculating formula.

pending on the mass number ( $A_B$ ) of the recoil nuclide for  $(n,2n)$ ,  $(n,\alpha)$ ,  $(n,p)$  and  $(n,np)$  reactions has been demonstrated. For the same material, according to the experimental results,  $(n,\alpha)$  reaction gives the largest reduced sputtering yield and  $(n,2n)$  gives the lowest ones. For some reactions, the present results have larger differences than those of calculation, but they give a good test for the systematic prediction of theoretical calculation.

In order to give a more detailed comparison between the experimental results and theoretical ones, the  $RS_n$  for each reaction is plotted on separate figures. For the  $(n,2n)$  reaction, Fig. 6 shows the calculating results agreeing with the experimental ones in the range of  $A_B$  from 40 to 70 and larger than the experimental ones for  $A_B$  from 90 to 220. For the  $(n,\alpha)$  reaction, calculating results have the same trend varied with  $A_B$  as that of the experiment, but about three times larger than that of the experiment as shown in Fig. 7. For the  $(n,p)$  reaction, the calculating results are in agreement with that of the experiment in the range of error as shown in Fig. 8. For the  $(n,np)$  reaction, the experimental results are obtained only for four reactions and two of those agree with the calculating results as shown in Fig. 9.

The experimental  $RS_n$  has the same systematics that the theoretical result gave in the formula (10) but with different fitting parameters  $a$  and  $b$ , which are given in Table III.

#### IV. A UNIVERSAL REVISED CALCULATING FORMULA

The ratios between the calculating results and the experimental results  $C/E$  are shown Fig. 10. It shows the ratios  $C/E$  vary from 0.5 to 6 depending on the type of reactions and the mass number of the recoil nuclides. For all four kinds of reactions, the values of  $C/E$  increase with increasing of  $A_D$ .

Sputtering processes induced by fast neutrons is a complicated process of collision cascade. Usually this process is different from the sputtering process induced by ions. The creation of primary knock on atoms by the incident neutrons not only can occur by elastic and inelastic collisions, but also by neutron reaction such as  $(n,\gamma)$ ,  $(n,2n)$ ,  $(n,p)$  and  $(n,\alpha)$ , or by fission processes. Reaction  $Q$  values and cross sections of incident neutrons with target atoms are very important

factors affecting sputtering yields. Moreover, energy spectra and angular distributions of sputtering atoms, the surface potential of target materials and property of materials such as single crystal or anneal material also will affect sputtering results. In order to find a convenient formula to calculate sputtering yields induced by fast neutrons, we introduce a revised parameter  $K$  in formula (7). We sign  $(RS_n)_{rev}$  as the revised  $RS_n$ . Therefore, the revised calculating formula is given as follows:

$$(RS_n)_{rev} = \left( \frac{63}{Z_D^{1.33}} - \frac{98Z_D^{1.27}}{Z_D^{1.98}} \right) N \langle R \rangle. \quad (11)$$

All results are calculated again using formula (11) and compared with the experimental  $RS_n$  values. New  $C/E$  values have had a great improvement. The new calculating results for most reactions are in agreement with experimental results in the range of 50% approximately as shown in Fig. 11. Therefore, the reduced sputtering yields can be good predictors using the revised calculating formula (11) for four kinds of reactions. Moreover, as a good approximation, this formula can predict  $RS_n$  of other reactions, for example,  $(n,d)$ ,  $(n,t)$ ,  $(n,n\alpha)$  reactions, etc. Based on this result, we can further estimate some sputtering yields of important materials or alloys, especially for those in which the recoil nuclides with no activities, can be deduced.

#### V. CONCLUSIONS

We have made a study of the sputtering of radioactive recoil nuclides induced by fast neutron nonelastic reactions. Based on the theoretical calculation, a systematics of  $RS_n$  depending on the mass number of sputtering atoms is found for four kinds of reactions  $(n,2n)$ ,  $(n,p)$ ,  $(n,\alpha)$  and  $(n,np)$ . These systematics have also been demonstrated by the experimental measurements. A revised calculating formula is deduced by introducing a revised factor to predict reduced sputtering yield induced by fast neutrons.

#### ACKNOWLEDGMENT

Research work was performed under the funds for the returned scientists of USTC and CAS.

- <sup>1</sup>O. K. Harling, M. T. Thomas, R. L. Brodzinski, and L. A. Rancitello, J. Appl. Phys. **48**, 4328 (1977).
- <sup>2</sup>G. Cambi, D. G. Cepraga, S. Ciattaglia, L. D. Pace, and G. Cavallone, Fusion Eng. Des. **29**, 207 (1995).
- <sup>3</sup>C. Garcia-Rosales, J. Nucl. Mater. **211**, 202 (1994).
- <sup>4</sup>M. Kaminsky and S. K. Das, J. Nucl. Mater. **60**, 111 (1976).
- <sup>5</sup>R. Behrisch, R. Gahler, and J. Kalus, J. Nucl. Mater. **53**, 183 (1974).
- <sup>6</sup>L. H. Jenkins, G. J. Smith, J. F. Wendelken, and M. J. Saltmarsh, J. Nucl. Mater. **63**, 438 (1976).
- <sup>7</sup>M. Kaminsky and S. K. Das, J. Nucl. Mater. **53**, 162 (1974).
- <sup>8</sup>T. S. Baer and J. N. Anno, J. Appl. Phys. **43**, 2453 (1972).
- <sup>9</sup>R. Behrisch, Nucl. Fusion **12**, 695 (1972).
- <sup>10</sup>M. T. Robinson, J. Nucl. Mater. **53**, 201 (1974).
- <sup>11</sup>O. K. Harling, M. T. Thomas, R. L. Brodzinsky, and L. A. Rancitelli, Phys. Rev. Lett. **34**, 1340 (1975).
- <sup>12</sup>*Sputtering by Particle Bombardment II*, edited by R. Behrisch (Springer, Berlin, 1983), p. 217.
- <sup>13</sup>P. Sigmund, Phys. Rev. **184**, 383 (1969).
- <sup>14</sup>H. E. Schott, Radiat. Eff. **6**, 107 (1970).
- <sup>15</sup>B. J. Ye, Y. Ikeda, and Y. Kasugai, IAERI Research, 97-082, 1997.